18B.2 USING THE TLS TO IMPROVE THE UNDERSTANDING OF ATMOSPHERIC TURBULENT PROCESSES

Florence Bocquet [1](*), Ben B. Balsley [1], Michael Tjernström [2] and Gunilla Svensson [2]
([1]) Cooperative Institute for Research in Environmental Sciences, University of Colorado, Boulder, USA.
([2]) Department of Meteorology at Stockholm University, Sweden.

1. ABSTRACT

Our analyses of the dissipation rate of kinetic energy (ε) as a proxy for turbulence using a custom-built Tethered Lifting System (TLS) are directed towards improving our understanding of atmospheric turbulent processes. This technique can be used over a range of environmental conditions, locations, and spatial and temporal resolutions with the expectation that insights from such measurements will be used to improve parameterizations in regional and global climate models.

When comparing TLS measurements of ε to tower measurements of turbulence (by means of the vertical velocity variance σ_w^2), data appear to be well correlated. These results show that a) even in the most stable boundary layer, a "residual" turbulence is always present, b) measurements of ε in the nocturnal stable boundary layer show values as low as about 10^{-7} m^2 s^{-3}, and c) ε observations are useful even at low turbulence levels.

Keywords: turbulence dissipation rate, stable boundary layer.

2. INTRODUCTION

Turbulence is the major process controlling exchanges of energy and matter between the planetary boundary layer and the surface. Understanding atmospheric turbulent processes has been the subject of considerable research. Understanding turbulent processes in stable boundary layers remains particularly challenging because a) turbulence typically results from wind shear, and is probably affected by non-linear processes associated with atmospheric gravity waves (Fritts et al., 2003; Nappo, 2003), and b) suppressed mixing under stable conditions allows for small scale features to persist, hence complicating the flow dynamics. In very stable boundary layers, turbulence can be very weak and is often typically characterized by intermittent bursts of activity. Many aspects of the stable boundary layer dynamics are non-stationary, which require more sophisticated measurement and analysis techniques to sort out the relevant processes.

Studies related to understanding turbulence dynamics in the entire boundary layer are limited by the available data gathering methods. A discussion of current techniques and requirements for measuring stable boundary layer characteristics are briefly outlined in Balsley et al. (2006). Current methods include: boundary layer radars, frequency modulated continuous wave (FMCW) radars, Doppler and non-Doppler lidars, sodars, radiosondes, tethered balloons and kites, meteorological towers, and aircraft. As expected, each technique has advantages and disadvantages. For example, using meteorological towers, the vertical resolution of the measured turbulence is limited to the number of sensors mounted on the tower and to the tower height, which is typically less than 100 m. Hence towers provide neither data for a thorough vertical structure of the boundary layer nor the location and temporal change of the boundary layer top. Many authors (Arya, 1981; Beyrich, 1997; Seibert et al., 2000; Balsley et al., 2006) recommended a combination of at least two sensing techniques as the best tool for measuring the stable boundary layer turbulence and its top continuously and reasonably well.

Here, we present observations taken with a particular technique, namely the Tethered Lifted System (TLS), which is aimed at providing high temporal and vertical resolution data. The TLS is capable of taking measurements up to altitudes above the boundary layer and operating over a wide range of environmental conditions and locations. In order to both comprehend and appropriately model turbulent processes under stable atmospheric conditions, it is important to better understand the turbulence structure and dynamics of the boundary layer. The Cooperative Atmosphere-Surface Exchange Study (CASES-99) campaign provides support towards this goal. The present study is focused on a comparison between the kinetic energy dissipation rate ε from the TLS and tower measured measurements of σ_w^2.

(*) *Corresponding author address:* Florence Bocquet, CIRES, Univ. of Colorado, Boulder, CO. (303) 492-6748; bocquet@colorado.edu

3. CAMPAIGN, EXPERIMENTAL SYSTEM, AND DATA

The CASES-99 campaign was a nighttime experiment designed to study the stable boundary layer and the physical processes associated with its development, sustainability, and decay. This nearly one-month long campaign (5-31 October 1999) took place near Leon, Kansas, about 50 km east of Wichita, Kansas, and consisted of a significant deployment of surface, airborne, and remote sensing instruments (Poulos et al., 2002). One of these instruments was the Tethered Lifted System TLS (Balsley, 2008).

The TLS technology consists of lifting a kite or aerodynamic balloon (depending on wind speeds) by a tether line, on which lightweight instruments are mounted (Figure 1). Up to five groups of instruments (payload) can be suspended at regular intervals. Each payload consisted of a hot- and cold-wire sensor that recorded 200-Hz fluctuations of wind speed and temperature, respectively, as well as conventional low-frequency sensors collecting mean wind speed, temperature, and ambient air pressure.

In profiling mode, the TLS can reach up to 1-2 km in altitude, which is typically well above the stable boundary layer, i.e. in the residual layer. By profiling from one atmospheric layer to the other, it is possible to clearly identify the top of the boundary layer (Balsley et al., 2006).

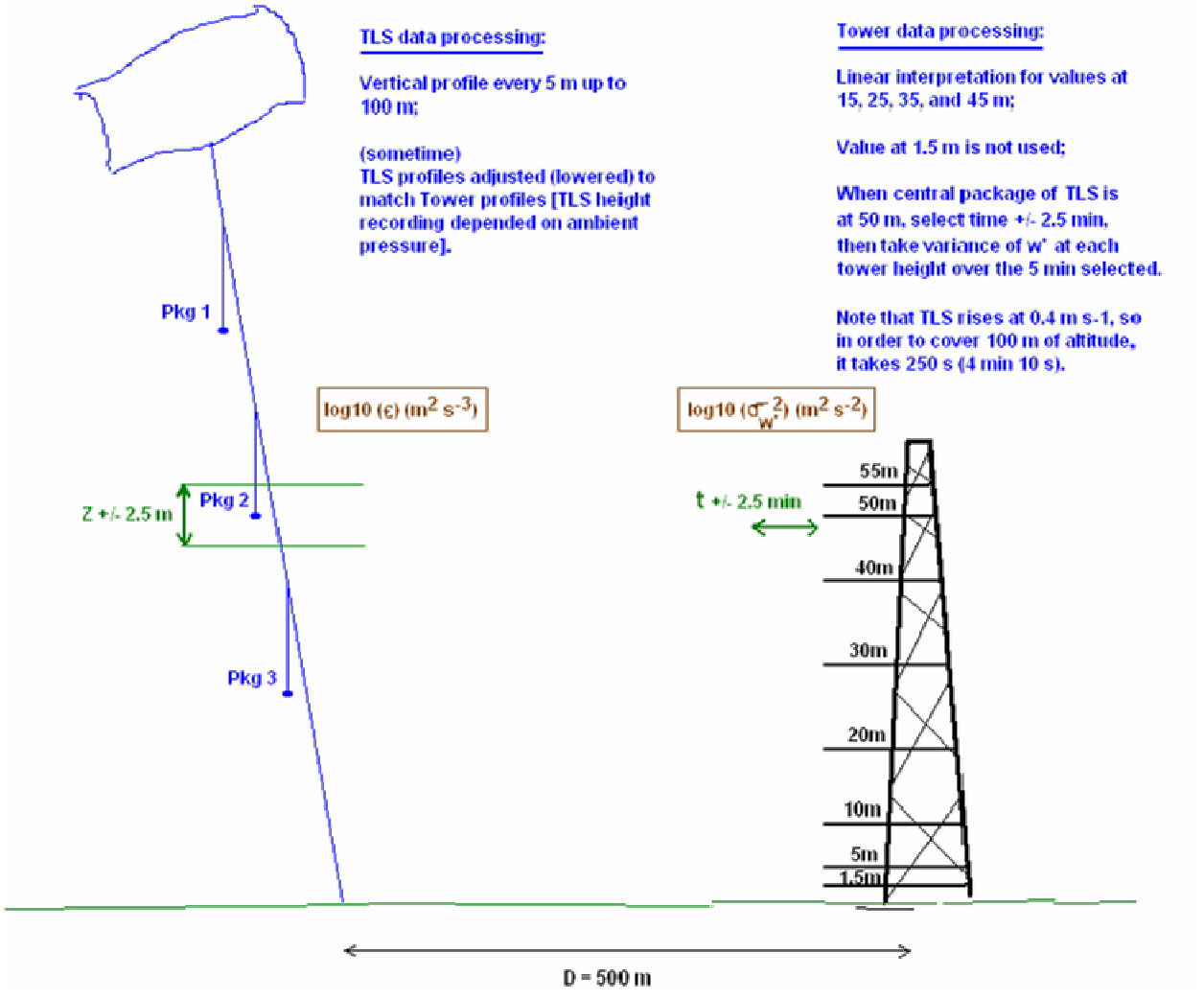

Figure 1
Schematic of the TLS and tower data processing used in the comparison of the two turbulent quantities, ε ($m^2 s^{-3}$) and σ_w^2 ($m^2 s^{-2}$), respectively.

4. EPSILON MEASUREMENTS USING THE TLS

High-temporal resolution turbulent kinetic energy dissipation rate (ε) and temperature structure constant (C_T^2) are inferred from the 200-Hz hot- and cold-wire probe data, respectively. Calibration procedures are described in Frehlich et al. (2003). One advantage of using ε instead of turbulent kinetic energy (TKE) is the relative insensitivity to the well-known problems in studying stably stratified flows that are, stationarity and locality (Vickers and Mahrt, 2003). The turbulence proxy parameter ε data are then given at a frequency of 1 Hz.

Estimates of ε obtained by the TLS hot-wire packages are calculated from the King's law and the inertial dissipation method based on Kolmogorov's hypothesis (Champagne et al., 1977). The accuracy of the resulting 1-sec ε values is determined by the accuracy of the slope of the calibration curve, which is typically better than 5% while the threshold for 1-sec ε estimates is about 10^{-7} m^2 s^{-3} (Frehlich et al., 2003).

The frequency of occurrence of all 1-sec values of ε collected during the entire campaign shows a range of values from about 5 x 10^{-2} to 10^{-7} m^2 s^{-3} (see companion paper by Balsley et al.). Note that 80% of the ε values are comprised between 5 x 10^{-2} and 5 x 10^{-6} m^2 s^{-3}, a dynamic range spanning 4 orders of magnitude. Figure 2 presents a subset of averaged ε data, corresponding to the first 100 m of the ascents and descents of the TLS. The motive for using the first 100 m of the TLS data is to focus on the dynamics of the lower stable boundary layer and for the subsequent comparative analyses with the tower data. The span and behavior of the subset of ε data are comparable to the complete dataset, which is discussed in the companion paper by Balsley et al. (this issue). This subset is then used to illustrate the variability of ε values over time that occurs within the first 100 m of the boundary layer (Figure 3).

Successive ascents and descents are typically separated by about 30 min to an hour. Obvious changes in the average ε structure are visible on all days, within each day and from day to day. The variability within a day is particularly obvious during Flight 9 (Oct 20), which occurred in atmospheric conditions characterized as a traditional boundary layer (Banta et al., 2006). Interestingly, a) Flight 9 is one of the flights experiencing the largest variability per ascent/descent sections, reflecting the greatest change in turbulence activities within the first 100 m of each ascent/descent; b) Flight 9 recorded the weakest turbulence, i.e. in the order of 10^{-7} m^2 s^{-3}; and c) in the span of about 4 hours, Flight 9 recorded the greatest change in turbulence activities over time, from ~ 10^{-7} to 10^{-2} m^2 s^{-3}.

The day to day variability is remarkable in the sense that the magnitude of ε relates to the boundary layer type. Flight 7 (Oct 14) and Flight 10 (Oct 21) are characterized by an upside-down boundary layer (Banta et al., 2002, 2006), and the first 100 m experienced relatively high ε values, in the order of 10^{-3} and 10^{-2} m^2 s^{-3}. Conversely, Flight 9 (Oct 20) and Flight 11 (Oct 23) are characterized by a traditionally formed boundary layer (Banta et al., 2006; Mahrt and Vickers, 2002), and the first 100 m experienced weak to moderate ε values, in the order of 10^{-5} to 10^{-3} m^2 s^{-3}. And when ε values were the weakest, in the order of 10^{-5} m^2 s^{-3}, as it is during Flight 8 (Oct 18), the boundary layer was characterized by a thin traditional boundary layer (Poulos et al., 2002). It is likely that mixing and turbulence brought down from a low-level jet (hence the upside-down boundary layer) have a much great impact on the boundary layer dynamics than when mixing and turbulence are building up in the traditional sense, i.e. from friction at the surface and thermal eddies.

To validate the temporal and spatial variability of these ε values (ε values obtained within the first 55 m above the surface of each ascent and descent of all flights), these TLS turbulence estimates were compared to turbulence measurements available from the "main tower", a 60-m tower located approximately 500 m away from the TLS operations (Figure 1).

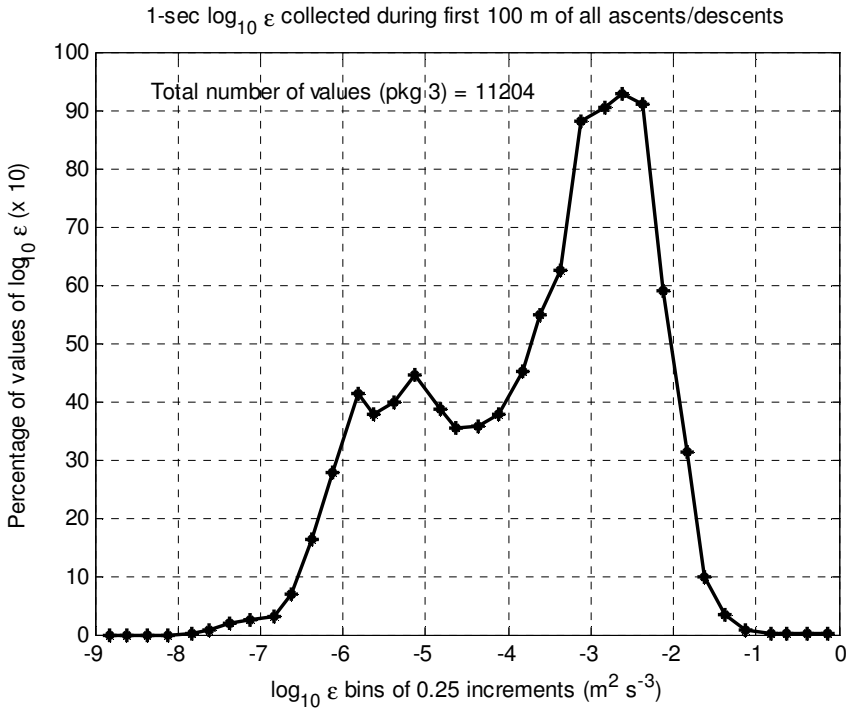

Figure 2
PDF (%) of 1-sec ε values collected by the TLS during the first 100 m of each ascent and descent. This PDF is for package 3, which has been arbitrarily selected. Values are presented using bins of log10 ε of 0.25 m^2 s^{-3} increments. Data have been scaled by multiplying all values by a factor of 10 for better display.

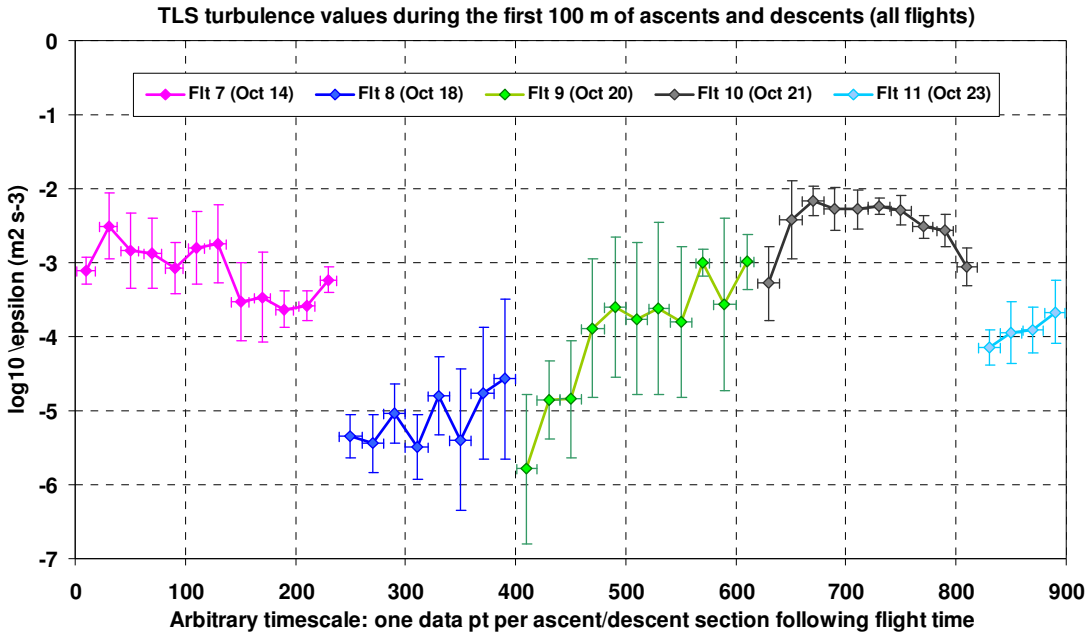

Figure 3
Average and standard deviation (variability bar) of log10 ε values over the first 100 m of each ascent and descent of the TLS. All flights are represented.

5. COMPARISON OF TLS ($\log_{10}$ ε) AND TOWER ($\log_{10}$ σ_w^2) TURBULENT QUANTITIES

The tower turbulence estimates are obtained from 3D sonic anemometers recording vertical wind speed at 11 different heights Z (every 5 m from 5 to 55 m) (Figure 1). One-sec averaged fluctuations in vertical wind speed, mathematically σ_w^2, and thereafter averaged over 5 min (i.e., T_Z - 2.5 to T_Z + 2.5 min, where T_Z is the time at height Z) were computed for comparison. Comparison with TLS turbulence proxy ε (averaged over 5 m in the vertical, i.e., Z - 2.5 to Z + 2.5 m) showed a R^2 value of 0.73 (Figure 4). Since ε is the dissipation rate of TKE in the atmosphere, and one of the components of the TKE equation is σ_w^2, it is no surprise that the two quantities are related and are behaving proportionally. The more turbulent energy is in the atmosphere, the greater the dissipation rate will be, and vice versa. Now, one question of interest is: how rapidly and easily does the energy dissipation rate adjust to the change of turbulent energy in the atmosphere?

A reasonable answer that would first explain the higher correlation between the two turbulence proxy quantities (Figure 4) may be that a relatively strong coupling exists, i.e. the stronger the turbulence, the shorter the time it takes for ε to adjust to the level of turbulence and hence to dissipate TKE, thus σ_w^2. Similarly, the scatter at low turbulence levels (Figure 4) may be explained by the fact that the weaker the turbulence, the longer and variable the time it takes for ε to adjust to the level of turbulence and to dissipate TKE, thus σ_w^2.

Particularly evident during Flights 8 and 9 is that slowly decreasing atmospheric stability, from being very stable to stable/near-neutral boundary layers (not shown), prevails. While capturing relatively weak turbulence (Figure 4), the associated relatively large variability bars (Figure 3) and the scatter of data points (Figure 4) clearly show this intermittent and burst-like activity of turbulence, characteristic of very stable boundary layers. The fact that at weaker turbulence levels, and in traditional-type of boundary layer (Flights 8, 9 and 11), the intermittent and burst-like activity of turbulence predominates, it allows for ε and σ_w^2 to capture the state of turbulence differently.

In addition, it is worth noting that weak turbulence (~ 10^{-7} m^2 s^{-3} for TLS turbulence) can be captured by both quantities, and that the TLS ε measurements are a valuable quantity over the range of turbulence levels, including weak turbulence in the order of 10^{-7} m^2 s^{-3}. Also worth mentioning is that weak turbulence, whether "residual" or background turbulence, is indeed present during these highly stable atmospheric conditions. This confirms the empirical notion that some turbulence activity is always present despite the highly stable conditions.

Interestingly, when displaying the same data sets as in Figure 4 in the form of probability density functions (PDFs), it appears that the turbulent kinetic energy as expressed by the peak in σ_w^2 centered at 10^{-2} m^2 s^{-2} is dissipated at a rate ranging from about 2.5 x 10^{-4} to 2.5 x 10^{-2} m^2 s^{-3} (Figure 5). Similarly, the much smaller peak of turbulent kinetic energy as expressed by the peak σ_w^2 around ~ 5 x 10^{-4} m^2 s^{-2} is dissipated at a rate ranging from about 10^{-6} to 2.5 x 10^{-4} m^2 s^{-3} (Figure 5). It is thus apparent that the rate of energy dissipation is scaled to the turbulent energy present in the atmosphere. It is quite noticeable that the energy dissipation rate adjusts to the magnitude of the turbulent energy; though the secondary peak in σ_w^2 is not scaled to the energy dissipation rate as the main peak in σ_w^2 is to its dissipation rate. This may show that additional turbulent energy must be present but yet is not captured by the σ_w^2 quantity*. As a consequence, this turbulent energy must be smaller than what 1-sec σ_w^2 can resolve. It is important to mention that one other possible reason could give the same observation, that is, if the time scale of advection is much larger than the averaging time used to calculate σ_w^2. In this event, the same air mass would be very slow to move passed the sensor of interest, resulting in small σ_w^2. Nonetheless, the observation mentioned above provides additional clues regarding 1) background/residual turbulence is always present, 2) background/residual turbulence may not be captured by the turbulence proxy σ_w^2, and 3) background/residual turbulence could be appropriately quantified when using the turbulence proxy ε.

Characterizing the structure and dynamics of the boundary layer is certainly a primary goal for scientists and climate modelers, but in order to achieve its most accurate representation in time and space, a number of requirements needs to be met. One of these requirements is that all significant dynamical characteristics of atmospheric turbulence are appropriately represented. One common mistake when undertaking such analyses is time-averaging.

* It should be kept in mind that the instrument limitation could also affect the σ_w^2 quantity, and more so when σ_w^2 becomes smaller.

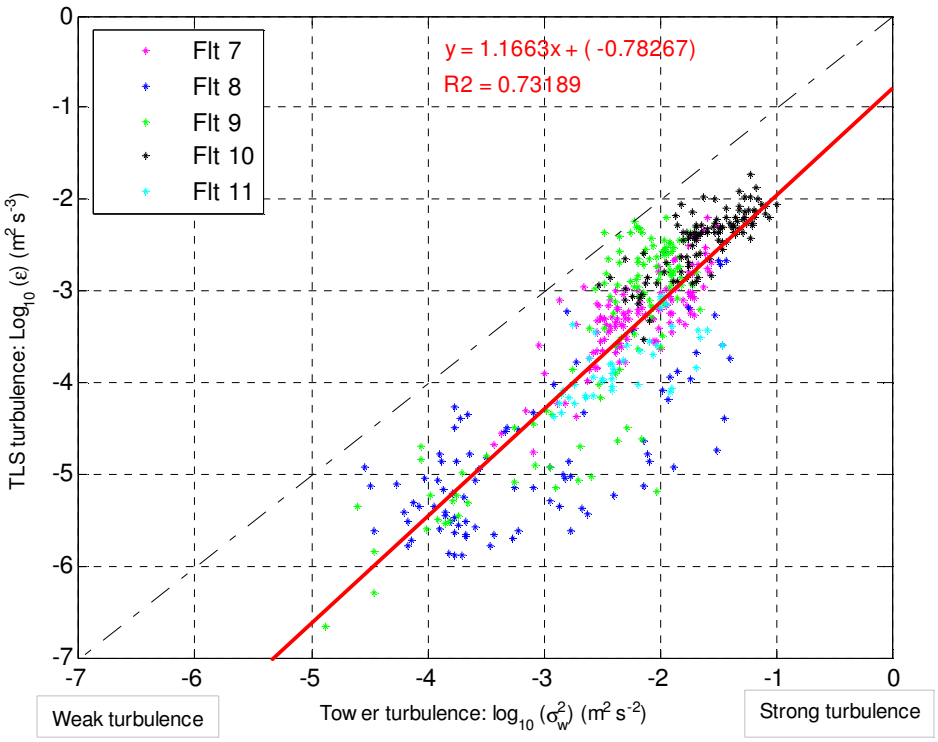

Figure 4
Correlation between tower turbulence expressed by log10 σ_w^2 (m^2 s^{-2}) and TLS turbulence proxy expressed by log10 ε values (m^2 s^{-3}). The first 100 m of all ascents and descents from each flight are represented.

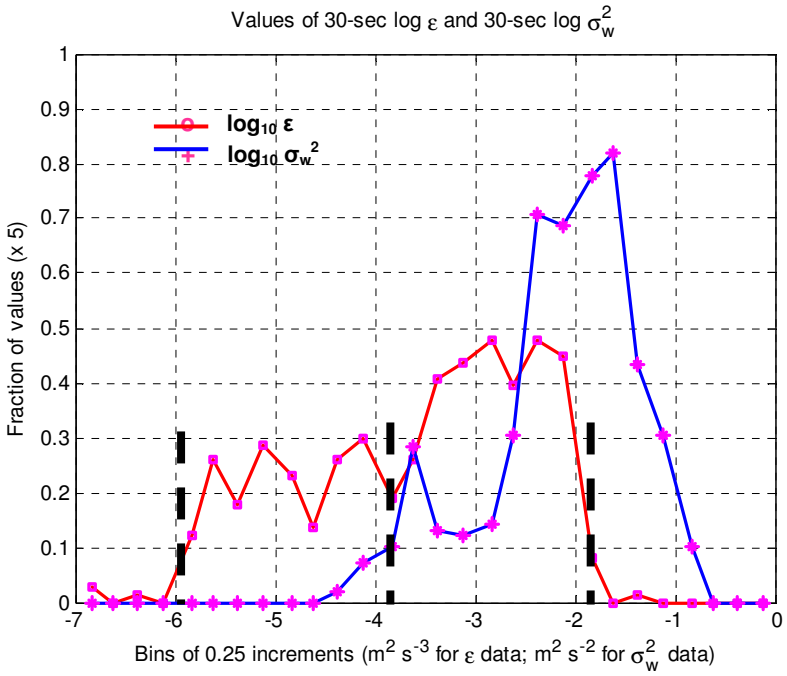

Figure 5
The figure presents the PDFs of TLS log10 ε data and tower log10 σ_w^2 data binned by increments of 0.25 m^2 s^{-3} and m^2 s^{-2} respectively. The TLS data consists of the average ε values over the first 100 m of all flights. The tower data matches the TLS ascents and descents up to 55 m of altitude. Data have been scaled to 1 by multiplying all values by a factor of 5.

6. TIME-AVERAGING

Two problems arise with time averages: the choice of the time over which to average, and the representation of that average as estimate of the ensemble average. For example, it is important to ensure that all significant flux-carrying wavelengths are included.

Since the two compared quantities are different, i.e. σ_w^2 and ε represent two different parts of the spectrum, it is also of interest to analyze the quantities under different time-averages. Figure 6 presents two time-averaged PDFs for both TLS and tower turbulence proxies, which have been binned by increments of 0.25 $m^2\ s^{-3}$ and $m^2\ s^{-2}$ respectively. The averaging times for the tower turbulence proxy σ_w^2 are 5 and 30 sec. The TLS data under consideration again represent the first 100 m of each ascent and descent of all flights. The averaging times for the TLS turbulence proxy ε are calculated from the vertical displacement of the TLS. Vertical displacements of 2 and 12 m represent about 5 and 30 sec, respectively (at the TLS moving rate of 0.4 m s^{-1}).

Over the range of measured turbulence proxy ε, both 5- and 30-sec time-averaged PDFs behave very closely (Figure 6, top), showing that relevant turbulence scales are independent of these time averages. This behavior is expected since the link to scales is lost as a result of ε being estimated from the inertial sub-range. On the other hand, the 5- and 30-sec time-averaged PDFs for σ_w^2 values show slightly different PDFs. The difference is observed across the measured range of values (Figure 6, bottom). As a result, the two peaks are slightly shifted from one another or of slightly different magnitude. The behavior is also expected: the larger the time-average, the more the PDF is shifted towards larger values of σ_w^2, and vice versa. This occurs because more, or less, of the spectrum is included in the averaging. Though this difference is relatively small, hence is likely to not have any impact on further analysis. Nonetheless, this observation is to be taken with caution as results could differ when encountering different atmospheric conditions, different terrains, different instrumentation, etc.

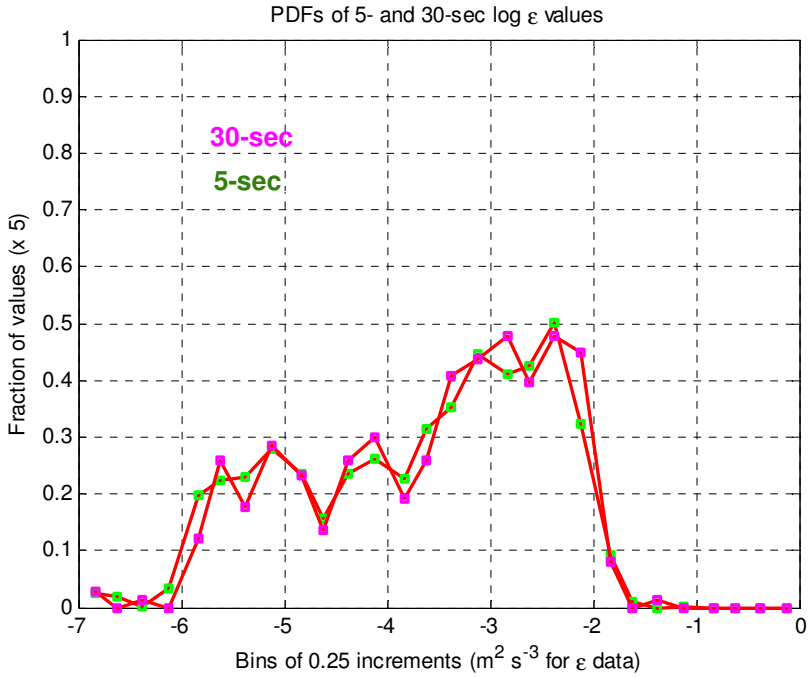

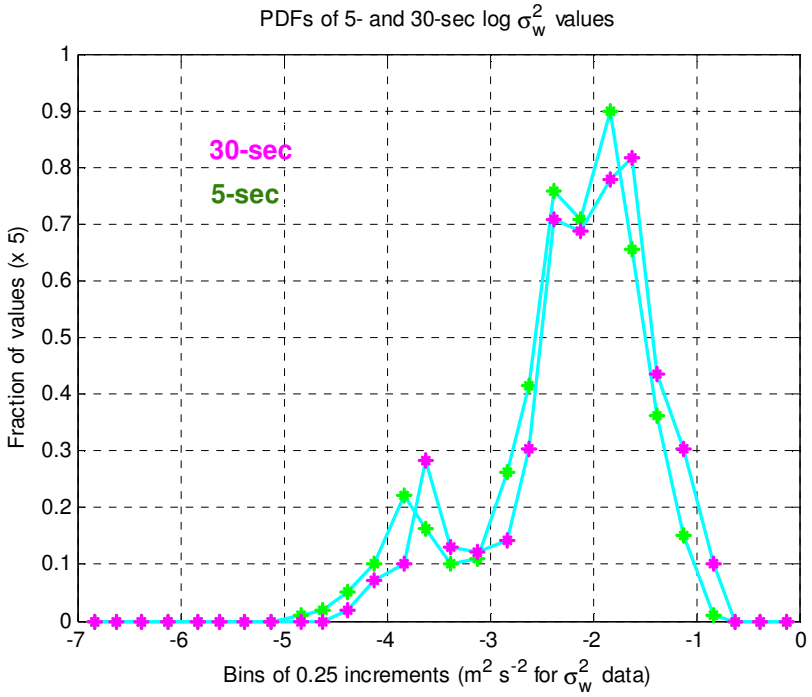

Figure 6
Two time-averages (5- and 30-sec) are used to calculate the density distribution profiles of TLS proxy turbulence log10 ε (top) and tower proxy turbulence log10 σ^2_w (bottom). Both y-axes have been scaled by a factor of 5 for better display.

7. CONCLUSION

The CASES-99 campaign provided the first use of the TLS loaded with turbulence proxy sensors. The capability of measuring the turbulent kinetic energy dissipation rate as a proxy for atmospheric turbulence is of great interest to field scientists as well as climate modelers. The comparison of this turbulence proxy measurements ε with the available tower wind fluctuations σ_w^2 showed great promises in this novel technique. With this novel technique, spatial and temporal characteristics of atmospheric turbulence and the dynamics present in the atmospheric boundary layer can be obtained.

This study showed that a) TLS turbulence proxy ε and tower turbulence proxy σ_w^2 are related, b) TLS turbulence proxy ε is capable of capturing small scale turbulence, such as background/residual turbulence, thus is better representative of the kinetic turbulent energy in the atmosphere, and yet c) TLS turbulence proxy ε is less sensitive to time-averaging than its tower counter-part (for 5- and 30-sec averages).

One of the next steps of this research is to characterize atmospheric turbulence such that the dynamical behavior of the boundary layer, and its interactions with the surface and the upper levels of the troposphere, can be better understood. This in turn will help in complementing and/or improving the parameterization of such dynamics in climate models. Also, further validation of the TLS data, for example against Lidar Doppler data also obtained during CASES-99, will be undertaken.

8. REFERENCES

Arya S. (1981) Parameterizing the height of the stable atmospheric boundary layer. *J. Applied Meteorol.*, **20**, 1192-1202.

Balsley B. et al. (2003) Extreme gradients in the nocturnal boundary layer: structure, evolution, and potential causes. *J. Atmos. Sci.*, **60**(20), 2496-2508.

Balsley B. et al. (2006) High-resolution in situ profiling through the stable boundary layer: examination of the SBL top in terms of minimum shear, maximum stratification, and turbulence decrease. *Bull. Amer. Meteor. Soc.*, **63**, 1291-1307.

Balsley B. (2008) The CIRES Tethered Lifted System: a survey of the system, past results and future capabilities. *Acta Geophysica*, **56**(1), 21-57.

Balsley B. et al. (this issue) Turbulence in the nocturnal boundary layer: highly-structured, strongly-variable, but ubiquitous. AMS 18th Symposium on Boundary Layers and Turbulence, Stockholm, Sweden, 9-13 June 2008.

Banta R. et al. (2002) Nocturnal low-level jet characteristics over Kansas during CASES-99. *Bound.-Layer Meteorol.*, **105**(2), 221-252.

Banta R. (2003) Relationship between low-level jet properties and turbulence kinetic energy in the nocturnal stable boundary layer. *J. Atmos. Sci.*, **60**, 2549-2555.

Banta R. et al. (2006) Turbulent velocity-variance profile in the stale boundary layer generated by a nocturnal low-level jet. *J. Atmos. Sci.*, **63**, 2700-2719.

Beyrich F. (1997) Mixing height estimation from sodar data: a critical discussion. *Atmos. Environ.*, **31**, 3941-3953.

Champagne F. et al. (1977) Flux measurements, flux estimation techniques, and fine-scale turbulence measurements in the unstable surface layer over land. *J. Atmos. Sci.*, **34**, 515-530.

Frehlich R. et al. (2003) Turbulence measurements with the CIRES Tethered Lifted System during CASES-99: calibration and spectral analysis of temperature and velocity. *J. Atmos. Sci.*, **60**(20), 2487-2495.

Fritts D. et al. (2003) Analysis of ducted motion in the stable nocturnal boundary layer during CASES-99. *J. Atmos. Sci.*, **60**(20), 2450-2472.

Mahrt L. and Vickers D. (2002) Contrasting vertical structures of nocturnal boundary layers. *Bound.-Layer Meteorol.*, **105**(2), 351-363.

Nappo C. (2003) Observations of gravity-wave modulated turbulence in the stable boundary layer during the CASES-99 field study. *Geophys. Res. Abstracts*, **5**, Abstract #01786.

Poulos G. et al. (2002) CASES-99: a comprehensive investigation of the stable nocturnal boundary layer. *Bull. Amer. Meteor. Soc.*, **83**, 555-581.

Seibert P. et al. (2000) Review and intercomparison of operational methods for the determination of the mixing height. *Atmos. Environ.*, **34**, 1001-1027.

Vickers D. and Mahrt L. (2003) The cospectral gap and turbulent flux calculations. *J. Atmos. Oceanic Technol.*, **20**, 660-672.